
Article:
Elshaarani, T, Yu, H, Wang, L et al. (7 more authors) (2020) Dextran-crosslinked glucose responsive nanogels with a self-regulated insulin release at physiological conditions. European Polymer Journal, 125. 109505. p. 109505. ISSN 0014-3057

https://doi.org/10.1016/j.eurpolymj.2020.109505

Dextran-crosslinked glucose responsive nanogels with a self-regulated insulin release at physiological conditions

Tarig Elshaarani[1], Haojie Yu[1*], Li Wang[1*], Long Lin[2], Nan Wang[1], Kaleem ur Rahman Naveed[1], Li Zhang[3], Yin Han[3], Shah Fahad[1], Ni, Zhipeng[1]

[1]State Key Laboratory of Chemical Engineering, College of Chemical and Biological Engineering, Zhejiang University, Hangzhou 310027, P.R. China

[2]Department of Colour Science, University of Leeds, Woodhouse Lane, LS29JT, Leeds, UK

[3]Zhejiang Institute of Medical Device Testing, Hangzhou 310018, PR China

Abstract:

Different glucose-responsive nanogels of *N*-isopropylacrylamide (NIPAM) and 4-(1,6-dioxo-2,5-diaza-7-oxamyl) phenylboronic acid (DDOPBA) were synthesized using dextran-grafted maleic acid (Dex-MA) as a crosslinker. The formed nanogels (P(NIPAM-co-Dex-co-DDOPBA)s) were verified by ^{1}H NMR, TEM, DLS and X-ray photoelectron spectroscopy (XPS). The incorporation of DDOPBA provided a remarkable sensitivity towards glucose in physiological pH due to the existence of electron-withdrawing group in its structure. Similarly, the hydrophilic Dex-MA modulated the temperature-sensitivity near physiological temperature. The nanogels exhibited high insulin loading capacity and encapsulation efficiency and the *in vitro* release profiles demonstrated a glucose dependant release of the payload at physiological pH and temperature.

Keywords: Nanogel, Dextran, Glucose sensing, Insulin delivery

*Correspondence to Haojie Yu, E-mail: hjyu@zju.edu.cn. and Li Wang,E-mail:opl_wl@dial.zju.edu.cn

Tel: +86-571-8795-3200 and Fax: +86-571-8795-1612

1. Introduction

Diabetes mellitus is a rising health concern in recent years. The treatment of diabetes involves a frequent injection of exogenous insulin to regulate blood's glucose concentration to its normoglycemic level. However, the regular injections not only compromise the patient's quality of life but also fail to precisely maintain the optimum dose of insulin, leading to chronic complications of diabetes. It is desirable to develop an improved treatment for diabetes that meets the patient's physiological and lifestyle requirements [1-3]. One possible route to developing an improved treatment is based on the use of polymeric nanogels. Nanogels are small size hydrogel particles that consist of a physically or chemically crosslinked polymer chains. Nanogels that are responsive to *p*H, temperature, analyte and ionic strength have attracted considerable attention due to their applications in drug regulation systems. Their nano-size allows ease of functionalisation and administration via injection [4] and renders nanogels the ability to change their size in response to specific external stimuli rapidly. Phenylboronic acid (PBA)-based polymeric nanogels are considered as appropriate alternative insulin delivery systems. PBS has been considered as a synthetic mimic to lectins because of its ability to bind with biologically relevant 1,2- and 1,3-diols, such as saccharides, or with polyols formation of boronate esters. This binding is very useful for preparing PBA-based gels with dynamic covalent or responsive behavior [5]. Clearly, glucose-responsive nanogels to be used in insulin delivery systems should be biocompatible and applicable under physiological conditions. However, PBA-based nanogels are still at a distance from being clinically applicable. Thus, the response under physiologically relevant conditions remained an obstacle [6, 7]. Previously, an injectable nanogel was prepare to serve as a glucose-induced insulin delivery system [8]. However, the response of nanogels to glucose at physiological conditions is very low due to the high pKa of 3-acrylamido phenylboronic acid (AAPBA) and the influence of the microenvironment on AAPBA [9].

Many strategies have been employed to match the pKa of the glucose-responsive moieties to the physiological *p*H [10-12] this includes using different PBA derivatives [13-15]. For instance, introducing carbamoyl as an electron-withdrawing group into the phenyl ring reduces the pKa of the synthesized 4-(1,6-dioxo-2,5- diaza-7-oxamyl) phenylboronic acid (DDOPBA) to 7.8, which is quite close to physiological *p*H [16]. Thus, a rational design can provide polymers-bearing PBA capable of serving for insulin delivery systems. That is, the formation of boronate anions via PBA-glucose complexation can provide a simultaneous change in the material properties and morphology. As an example, the binding of glucose to PBA-based thermoresponsive hydrogels can increase the hydrophilicity of the hydrogel, provoke hydrogel's swelling, increase the pore size and hence accelerate the drug diffusion through the network [16]. Another challenge encountered PBA-based nanogels is biodegradability. Therefore, incorporating a biodegradable and biocompatible monomer, polymer or crosslinker can endow PBA-based polymers a biodegradable nature. Dextran is biodegradable and biocompatible polysaccharides that are commonly used in medical applications [17-19]. The availability of hydroxyl groups in their structures provide them with the biocompatibility and applicability in the *in vivo* environment with no inflammatory response, and their chemical structures provide them with long term stability. Furthermore, the hydroxyl groups in their structures can be modified under different conditions for further crosslinking [20-22] or attachment of bioactive molecules or specific functional groups [23, 24].

In this work, injectable nanogels were synthesized to overcome the shortcoming of using AAPBA. Here DDOPBA was due to its relatively low pKa and the stability of its boronate anion at different temperatures. To accomplish our goal, DDOPBA was synthesized and crosslinked with NIPAM using pre-synthesized dextran-grafted maleic acid (Dex-MA) to prepare poly(N-isopropyl acrylamide-*co*-dextran-grafted maleic acid-*co*-4-(1,6-dioxo-2,5-

72 diaza-7-oxamyl) phenyl boronic acid)s (P(NIPAM-*co*-Dex-*co*-DDOPBA)) nanogels. Dex-
73 MA will possibly endow the prepared nanogels the biodegradability and modulated the
74 optimum temperature for glucose sensing to the physiologically relevant temperature by
75 tuning the VPTT of the nanogels. The responsivity of the prepared nanogels to glucose under
76 different temperatures was examined and the insulin release profiles were studied.

77 2. Materials and methods

78 2.1. Materials

79 Dextran (40 kDa) was purchased from Aladdin Ltd. 4-Carboxyphenylboronic acid (CPBA),
80 thionyl chloride, fluorescein isothiocyanate, crystalline porcine insulin and ammonium
81 persulfate (APS) were supplied by *J&K* chemicals. Dimethtlformamide (DMF) was dried
82 using activated 4ºA-type molecular sieves. After that, it was refluxed over potassium under
83 nitrogen atmosphere. Isopropyl alcohol is analytical reagent. Lithium chloride (LiCl) was
84 purchased from TCI Chemical. Ethylenediamine (EDA) was supplied by Sinopharm, China
85 and dried with molecular sieves for three days. Then, it was refluxed with calcium hydride
86 (CaH_2) for 8 h and distilled under vacuum.

87 2.2. Synthesis of 4-(1,6-dioxo-2,5-diaza-7-oxamyl) phenylboronic acid (DDOPBA)

88 The synthesis of DDOPBA was based on the three-step method reported by Kataoka [9]. In
89 this method, 4-carboxyphenylboronic acid (CPBA) (5.036 g, 30.15 mmol) was allowed to dry
90 under vacuum for 24 h. Then, the flask that contains the product was degassed using Ar gas
91 before adding thionyl chloride (75 mL, 1.05 mol). The suspension was stirred under the inert
92 atmosphere at 90 ºC for 24 h. Then, the excess amount of thionyl chloride was evaporated
93 under vacuum to yield 4-(chloroformyl) phenylboronic acid as white solids. The flask was
94 filled again with Ar gas, and the product was suspended in THF (60 mL). The suspension was
95 cooled in ice-path before being added dropwise to a pre-cooled mixture containing distilled

96 EDA (100 mL, 1.5 mmol) and TEA (5 mL, 35.95 mmol). The reaction mixture was allowed
97 to continue for 20 h at 0 °C, afterward, the excess EDA was evaporated. To the residue, 100
98 mL of ultrapure water was added. Then, the pH of the solution was adjusted to 4 using 1N
99 HCl. The white precipitate that formed was filtered off, and the filtrate was concentrated and
100 stored overnight at 4 °C to produce a white crystalline product, namely, 4-[(2-
101 aminoethyl)carbamoyl] phenylboronic acid (AECPBA). The product was recrystallised twice
102 in water and yielded 2.103 g which was 42% of CPBA.
103 In the last step, AECPBA (1.200 g, 9.12 mmol) was dissolved in 48 mL freshly prepared
104 NaOH (1 N). The solution was degassed and cooled in the ice-water path. After that, chilled
105 acryloyl chloride (1.56 mL, 17.28 mmol) was added in a drop-wise manner while stirring for
106 24 h. The resulting solution was concentrated, and then its pH was adjusted to 4 and kept
107 overnight at 4 °C to form a white crystalline solid. The product was recrystallised in water
108 and left to dry in oven at 40 ºC to yield DDOPBA.

109 **2.3. Synthesis of Dextran-grafted maleic acid (Dex-MA*)***

110 Dex–MA was synthesised according to a previously reported method [20]. Briefly, Dextran
111 (5.012 g, 0.125 mmol) was dissolved in 20 mL DMF in which 2.001 g LiCl was previously
112 dissolved. The mixture was stirred at 90 °C under Ar atmosphere for 40 min, then the
113 temperature was decreased to 60 °C, and TEA (64 µL, 0.46 mmol) was added as a catalyst.
114 After stirring for a further 15 min, maleic anhydride (4.030 g, 41 mmol) was added slowly to
115 the solution, and the reaction was continued for 10 h under Ar atmosphere. Then, the final
116 product was precipitated in 50 mL of cold isopropyl alcohol, filtered and washed three times
117 with isopropyl alcohol. The product (Dex–MA) was placed in a vacuum oven at ambient
118 temperature for two days to dry and stored in a cold dark for subsequent reaction.

119 **2.4. Preparation of glucose-responsive nanogel**

120 P(NIPAM-co-Dex-co-DDOPBA) nanogels have been prepared according to the method
121 described by Zhang et al [25]. Nanogels with different DDOPBA loadings were fabricated. In
122 a typical method, DDOPBA (68.2 mg, 0.25 mmol) was dissolved in 20 mL ultrapure water
123 and degassed for 30 min. Then, NIPAM (280.7 mg, 2.5 mmol), SDS (22.8 mg, 0.092 mmol)
124 and Dex-MA (130.2 mg, 0.003 mmol) were added. The mixture was stirred, passed through
125 45 µm filter into a three-necked flask, and degassed for 10 min. Then, the filtered solution
126 was heated to 70 °C and maintained at that temperature for 1 h. Subsequently, APS (13.4 mg,
127 0.06 mmol) was added to initiate the reaction. The resulting solution was allowed to
128 polymerize for 8 h and the resulting nanogel was placed in dialyses bags (8000-14000
129 MWCO) and exhaustively dialyzed against water for 7 days to remove the unreacted
130 monomers and surfactant. Then, the purified nanogel was lyophilized to obtain the dried
131 nanogels. The control nanogel P(NIPAM-*co*-DDOPBA) (NG0) was prepared by dissolving
132 DDOPBA (67 mg, 0.25 mmol) in 20 mL ultrapure water, after dissolution and DDOPBA
133 solution was degassed for 30 min. then, NIPAM (383.4 mg, 25 mmol), SDS (11.7 mg, 0.06
134 mmol) and MBA (11.6 mg, 0.075 mmol) were added and the mixture was stirred to get
135 dissolved. After dissolution, the reaction mixture was filtered, degassed for 10 minutes and
136 heated at 70 °C for 1 h. The heated solution was initiated by APS (11.7 mg, 0.06 mmol) and
137 kept stirring at these conditions for 8 h to get the control nanogel. The nanogel was filtered
138 using dialysis bag with molecular weight cut off from 8000 to 14000.

139 **2.5. Characterisation**

140 **2.5.1 Dynamic light scattering**

141 The hydrodynamic radii (R_h) of the nanogels and their distributions were measured using a
142 Zetasizer Nano-ZS Malvern apparatus (Malvern Instruments Ltd) using disposable cuvettes.
143 The excitation light source was a He-Ne laser at 633 nm, and the intensity of the scattered

144 light was measured at 173°. The temperature of the medium was adjusted using a built-in
145 temperature controller. Before each measurement, the samples were filtered using a 0.45 µm
146 Millipore filter. The suspensions were allowed to equilibrate at each temperature for 10 min
147 before measurement to attain thermal equilibrium. Each sample was measured 3 times with
148 11 measurements each, and a 10 second acquisition time between them. The values recorded
149 here are the average of these measurements. This method measures the rate of the intensity
150 fluctuation and the size of the particles is determined through the Stokes-Einstein equation
151 [26].

152 **2.5.2 Transmission electron microscopy**

153 The morphology of the nanogels was investigated using transmission electron microscopy
154 (TEM). The freeze-dried nanogels were dispersed in phosphate buffered saline (PBS, pH 7.4,
155 0.01 M), sonicated for 10 min, and dripped onto a copper grid covered with a perforated
156 carbon film and allowed to dry at room temperature prior to measurements.

157 **2.5.3 Thermogravimetric analysis (TGA*)***

158 The thermal stability of the prepared nanogels was studied using a TA-Q500 (Mettler-
159 Toledo) under N_2 gas at a flow rate of 20 mL/min. A sample weight of 3-4 mg was heated
160 from 50 to 600°C at a rate of 10 °C/min and the variation in the nanogel's weight against
161 temperature changes (TGA data) and its first derivative [differential thermogravimetry (DTG)
162 data] was continuously collected.

163 **2.5.4 Volume phase transition temperature (VPTT)**

164 The VPTT was located by plotting the hydrodynamic radii (R_h) of the nanogels at each
165 temperature. DLS was used to determine the R_h at a scattering angle of $\theta = 174°$, to achieve
166 this, the nanogels were dispersed in media of different glucose concentrations prepared with
167 PBS (0.01M, 7.4 pH). Before measurement, each sample was filtered using a 45 µm filter. At

168 each measurement, the samples were allowed to equilibrate at the selected temperature for 10
169 min before measurement.

170 **2.5.5 Other characterisations**

171 Fourier transforms infrared (FTIR) spectra were measured on a Nicolet 7500 spectrometer
172 using the potassium bromide (KBr) method. The dried nanogels were analysed in the range
173 between 4000 and 500 cm^{-1} in an attempt to confirm the existence of the unsaturated double
174 bonds and compare their intensities. ^{1}H NMR spectrum was recorded on Agilent 600 NMR
175 spectrometer in dimethyl sulfoxide-d6 (DMSO-d6) or water (D_2O). X-ray photoelectron
176 spectroscopy (XPS) was performed on a VG ESCALAB MARK 11 XPS system.

177 **2.5.6 In vitro loading and release study**

178 The insulin loading capacity and association efficiency of the nanogels were determined by
179 mixing the dispersed nanogel (2 mg/mL) with 3 mL FITC-insulin (3 mg/mL) in PBS (0.01
180 M, *pH* 7.4. Then, the nanogel was incubated in a refrigerator at 4 °C for 24 hours. After that,
181 the nanogel was centrifuged (15000 rpm, 20 °C) for 30 min and the supernatant was extracted
182 to quantify the amount of the free insulin. The absorbance of the total insulin and the free
183 insulin was measured by UV spectrometer at 492 nm. The association efficiency (AE) and
184 the loading capacity (LC) of the nanogels were calculated using the following formula [8].

$$\text{AE}\ \% = \frac{\text{Total insulin} - \text{free insulin}}{\text{Total insulin}} \times 100\%$$

$$\text{LC}\ \% = \frac{\text{Total insulin} - \text{free insulin}}{\text{Nanogel weight}} \times 100\%$$

185

186 The insulin release was evaluated by determining the amount of the insulin released from the
187 insulin-loaded nanogel at different time intervals at 37 ± 0.5 °C using the Bradford method
188 [27]. At first, the insulin-loaded nanogels were dispersed into PBS having different glucose

concentrations (0, 1, and 3 mg/mL) and placed in a shaking incubator (100 revolutions/min) at 37 °C. After each time interval, the incubated tubes were centrifuged at a rate of 15000 rpm and 20 °C. The supernatant was collected and its absorbance was recorded. The nanogel was redispersed in fresh release medium for the next measurement. Non-loaded nanogel was used to calibrate the absorption of the nanogel. The insulin release was evaluated by determining the amount of the insulin released from the insulin-loaded nanogel at different time intervals at 37 ± 0.5 °C using the Bradford method [27]. At first, the insulin-loaded nanogels were dispersed into PBS having different glucose concentrations (0, 1, and 3 mg/mL) and placed in a shaking incubator (100 revolutions/min) at 37 °C. After each time interval, the incubated tubes were centrifuged at a rate of 15000 rpm and 20 °C. The supernatant was collected and its absorbance recorded. The nanogel was redispersed in fresh release medium for the next measurement. Non-loaded nanogel was used to calibrate the absorption of the nanogel.

3. Results and discussion

3.1. Synthesis and characterization of DDOPBA

DDOPBA was synthesized using a three-step method (Fig. S1), and the ^{1}H NMR confirmed the successful synthesis after each step (Fig. 1). The first step is the synthesis of 4-[(2-aminoethyl) carbamoyl) phenylboronic acid (AECPBA) by converting 4-carboxyphentlboronic acid (CPBA) to acid chloride (4-chlorocarbmol) phenylboronic acid. In this reaction, the hydroxyl group of the carboxylic group reacts with thionyl chloride to form chlorosulfite as intermediate, which act as leaving group. Then, the acid chloride reacts with ethylenediamine to form AECPBA. The chemical shifts of CPBA monomer were verified by 1H NMR (DMSO, 600 Hz) and they were as follow (Fig. 1a). δ: 7.7-8.3 [-CO-C_6H_4-$B(OH)_2$, 4H] and 12.8 [-COOH].

213 The successful synthesis of AECPBA, which was confirmed by using 1H NMR (D_2O, 600
214 Hz). δ: 3.2-3.6 [-HN-CH_2-CH_2-NH_2, 4H], 7.7 [-CO-C6H4-B(OH)$_2$, 4H] (Fig. 1b). Then,
215 DDOPBA was synthesised by reacting AECPBA with acryloyl chloride, and the structure
216 was studied using ^{1}H NMR using DMSO as a solvent (Fig. 1c). δ: 3.4 [-NH-C<u>H</u>$_2$-C<u>H</u>$_2$-NH-,
217 4H], 5.57-6.09 [C<u>H</u>$_2$=CH-CO-, 2H], 6.18 [CH_2=C<u>H</u>-CO-, 1H], 7.76-7.82 [-CO-C_6<u>H</u>$_4$-B(OH)$_2$,
218 4H], 8.13 [-CO-C_6H_4-B(O<u>H</u>)$_2$, 2H, and 8.2-8.5 [-N<u>H</u>-CH_2-CH_2-N<u>H</u>-, 2H] [9, 28].

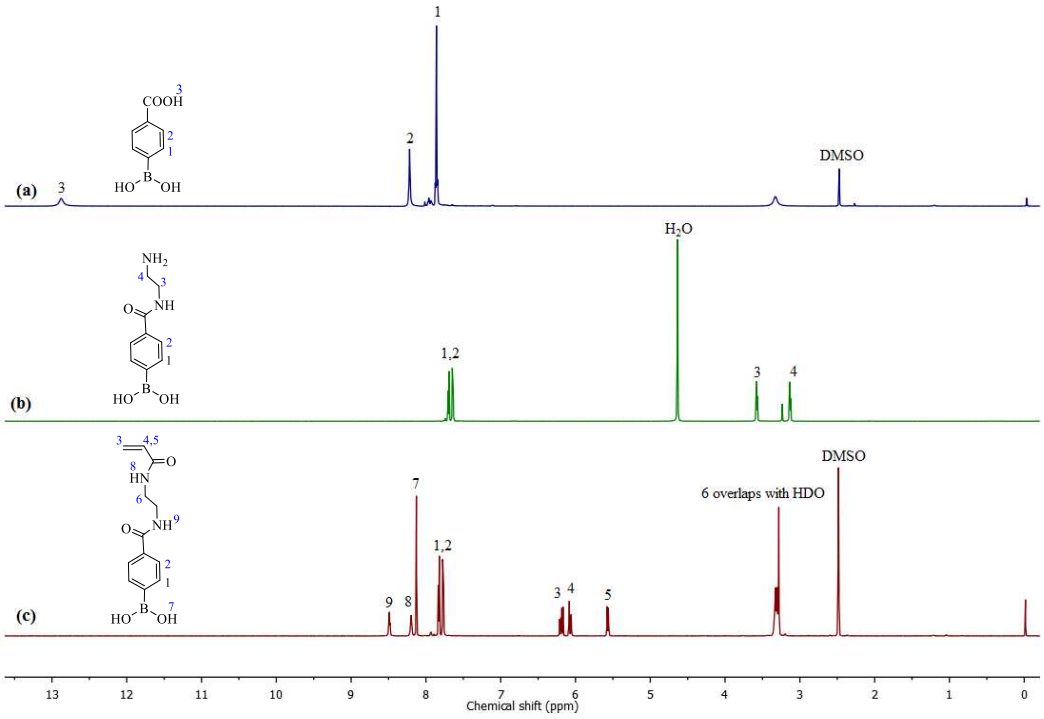

219

220 Fig. 1.^{1}H NMR spectra of (a) CPBA, (b) AECPBA, and (c) DDOPBA.

221 **3.2. Synthesis and characterization of Dex-MA**

222 Dextran has three hydroxyl groups per saccharide monomer, which can be functionalised
223 with maleic anhydride. The synthesis of Dex-MA is the condensation coupling reaction
224 between the hydroxyl groups of dextran and the anhydride groups of maleic anhydride. This
225 esterification reaction opens the ring of maleic anhydride to form a carboxylic acid end
226 group. The reaction was catalysed using triethyleneamine as a Lewis base to increase the
227 reactivity of the hydroxyl group of dextran. The scheme of the abovementioned reaction is
228 depicted in Fig. S2. The successful synthesis of Dex-MA was confirmed by FTIR spectra in

229 Fig. S3, as the existed peak at 1728 cm^{-1} in Dex-MA spectrum is the C=O stretching
230 vibrations resulted from the esterification reaction between dextran and maleic acid and from
231 the end group of maleic acid, this peak does not exist in the unmodified dextran. The broad
232 peak with the maximum at 3400 cm^{-1} is the -OH absorption band of the unreacted hydroxyl
233 groups in dextran and the carboxyl group of maleic acid. The peak at 2923 cm^{-1} is attributed
234 to the C-H stretching vibrations. The stretching bands of the -CH=CH- appeared at around
235 1667 cm^{-1} , and the peak at 824 cm^{-1} is for the C=C-H bending vibrations [22].
236 ^{1}H NMR spectra of dextran and Dex-MA is shown in Fig. 2. Therein, the peaks in the range
237 of 3.4-3.9 ppm, which are in a similar position for dextran and Dex-MA, are attributed to the
238 protons attached to C_2-C_6 carbon atoms. The protons of the anomeric carbon (C_1) are shifted
239 downfield compared to the protons of C_2-C_6,and appeared at 4.8-5.2 ppm due to the direct
240 attachment of C_1 to two oxygen atoms [21]. Distinctive peaks of Dex-MA were observed in
241 the range of 6.2-6.5ppm, which were assigned for -CH=CH- (C_7 and C_8) adsorption bands.

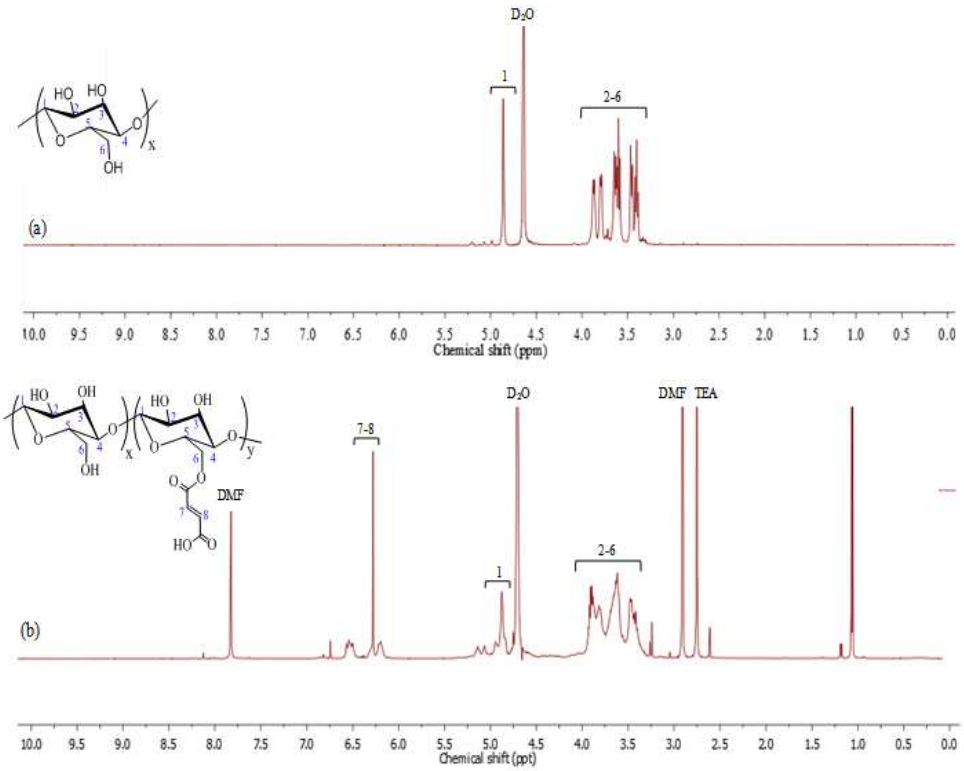

242

243 Fig. 2.^{1}H NMR spectra of (a) dextran and (b) Dex-MA.

244 The degree of substitution maleic anhydride on dextran (the number of MA groups in one
245 hundred anhydroglucose units) was calculated by dividing the integration area of the double
246 bond peaks of MA at 6.26 over the hydroxyl hydrogen peaks of dextran at 4.86. According to
247 the calculations, the DS of Dex-MA in (b) was 47 %.

248 **3.3. Synthesis and characterization of P(NIPAM-*co*-Dex-*co*-DDOPBA) nanogel**

249 The nanogels, named as NG1, NG2 and NG3 were prepared via free-radical precipitation
250 polymerization, which is a widely used method for preparing monodispersed spherical
251 particles with small size. Nanogels having different feeding ratios of DDOPBA and NIPAM
252 were synthesized. To endow the prepared nanogels biodegradability, Dex-MA was used as a
253 crosslinker. The feed chemical composition of the prepared nanogels is shown in Table 1 and
254 the reaction was schematically depicted in Scheme 1. The stepwise illustration of the
255 synthetic procedure is shown in Scheme 2. The FTIR spectra of the prepared nanogels are
256 presented in Fig. 3 and Table S1 listed the absorption bands of the existed functional groups**.**
257 Taking NG2 as an example, the peaks at 1380 cm^{-1} are due to the asymmetric vibrations of B-
258 O of phenylboronic acid and their corresponding symmetric vibrations located at 870 cm^{-1}
259 [29]. The peaks at 3420 cm^{-1} are attributed to the boronic acid, the N-H stretching vibration of
260 NIPAM, the unreacted -OH groups of dextran and the carboxylic acid. This peak is broad
261 owing to the interactions of polymer molecules with O-H vibrations of the non-freezing water
262 molecules [30]. The peak at 2961 cm^{-1} is the aliphatic CH_2 asymmetric vibrations. The peaks
263 of C=O stretching of amide 1 and N-H bending of amide 11 appeared at 1633 cm^{-1} and 1533
264 cm^{-1} respectively. The peak at 1633 cm^{-1} is larger when compared to that of dextran in Fig.
265 S3, and this is due to the immersion of -CO stretching of NIPAM in the same peak position
266 of amide 1.

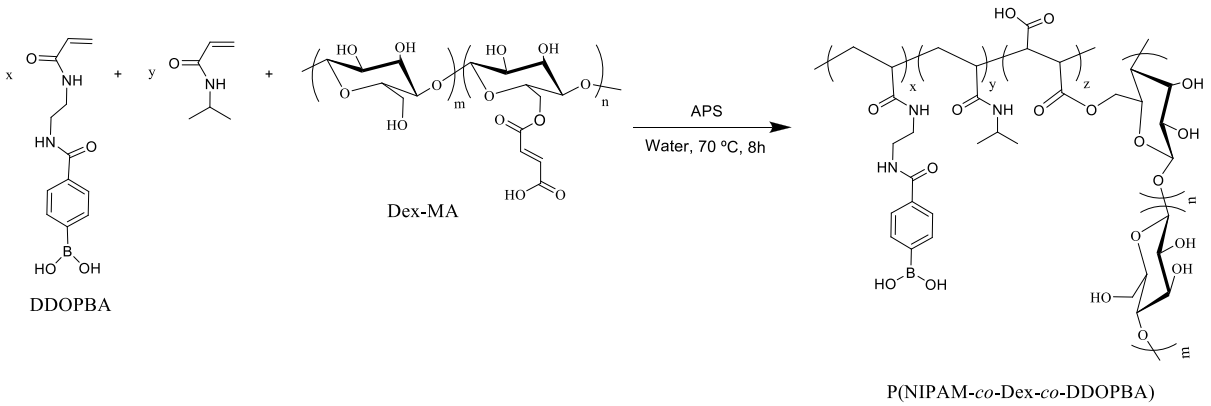

Scheme 1 Synthetic reaction for the synthesis of P(NIPAM-*co*-Dex-*co*-DDOPBA) nanogel.

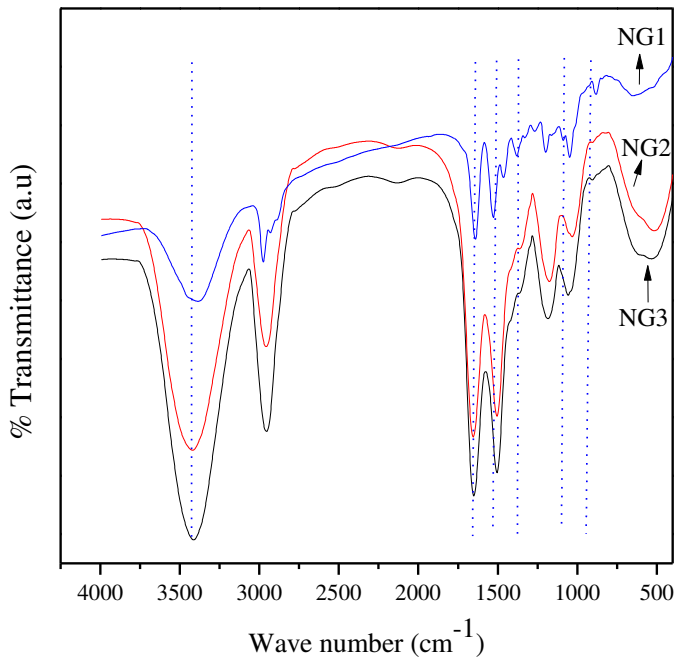

Fig. 3 FTIR spectra of P(NIPAM-*co*-Dex-*co*-DDOPBA) nanogels.

The broad peak at 1049 cm^{-1} assigned for -CO stretching and the hydroxyl group stretching vibration, which indicated the strong interaction between Dex-MA, DDOPBA and NIPAM monomers. It can be observed that the intensity of amide 1 bands is much higher compared to amide 11 due to the hydrogen bonding between NIPAM and Dex-MA [31, 22]. The C-H vibrations of the benzene ring appeared at 1380 cm^{-1} and the -C=C- vibrations of the benzene ring merged with the vibrations of the amide 11 vibrations at 1533 cm^{-1} [32].

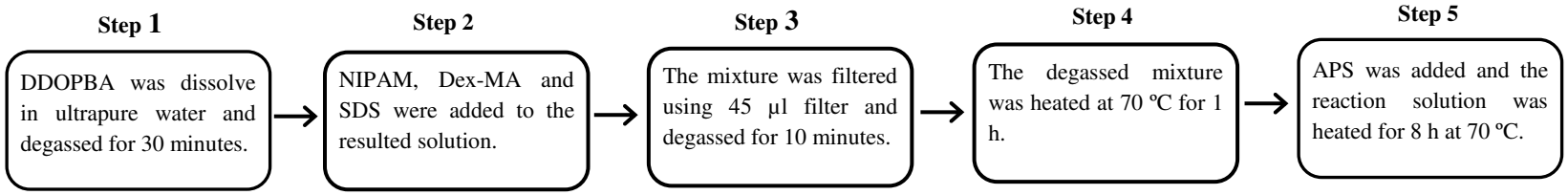

Scheme 2 Stepwise illustration for the synthetic procedure of P(NIPAM-*co*-Dex-*co*-DDOPBA) nanogels

Table 1 The synthetic details of P(NIPAM-*co*-Dex-*co*-DDOPBA) nanogels

	Step 1				Step 2							Step 3	Step 4		Step 5				
Samples[a]	DDOPBA (A)		Water	Ar purging	NIPAM (B)		Dex-MA (C)	sugar-units	SDS (D)		Ar purging	T	t	APS (E)		Molar ratio	T	t
	mg	mmol	mL	min.	mg	mmol	mg	mmol	mg	mmol	min.	h	ºC	mg	mmol	A: B: C: D: E	h	ºC
NG0	67.0	0.25	20	30	383.4	2.5	00.0	0.00	11.7	0.060	10	1	70	13.4	0.06	1: 10: 0.00: 0.24: 0.48	8	70
NG1	68.2	0.25	20	30	380.7	2.5	130.2	0.62	22.8	0.092	10	1	70	13.4	0.06	1: 10: 2.48: 0.37: 0.48	8	70
NG2	134.5	0.50	20	30	380.1	2.5	136.1	0.62	23.4	0.092	10	1	70	13.4	0.06	2: 10: 2.48: 0.37: 0.48	8	70
NG3	200.0	0.75	20	30	381.4	2.5	135.1	0.62	23.7	0.092	10	1	70	13.4	0.06	3: 10: 2.48: 0.37: 0.48	8	70

[a]NG0 stands for P(NIPAM-*co*-DDOPBA) nanogel; NG1, NG2 and NG3 stand for P(NIPAM-*co*-Dex-*co*-DDOPBA) with 10, 20 and 30 mol% DDOPBA, respectively.

*APS was dissolved in distilled water at a concentration of 13.4 mg/mL and injected to the reaction mixture.

The ^{1}H NMR spectra of the prepared nanogels are shown in Fig. 4 Similar to Dex-MA crosslinker, the ^{1}H NMR spectra of the nanogels at the range between 3.40-3.82 ppm are assigned to the C_2-C_6 carbon atoms of dextran. The chemical shift at 3.58 ppm is due to the [4H, -C$\underline{H}_2$-C$\underline{H}_2$-] protons of DDOPBA. The characteristic peaks of the phenyl ring [4H, -$C_6\underline{H}_4$-B$(OH)_2$] are shown at 7.2 ppm. The strong peak at 1.01 ppm is due to (9H, -C$\underline{H}_3$) protons of NIPAM [28]. While the peak at 1.39 ppm is due to (2H, -C$\underline{H}_2$) protons, the peak at 1.95 ppm is due to (1H, -C$\underline{H}$) protons, the peak at 7.8 ppm is due to (3H, -NH) protons.

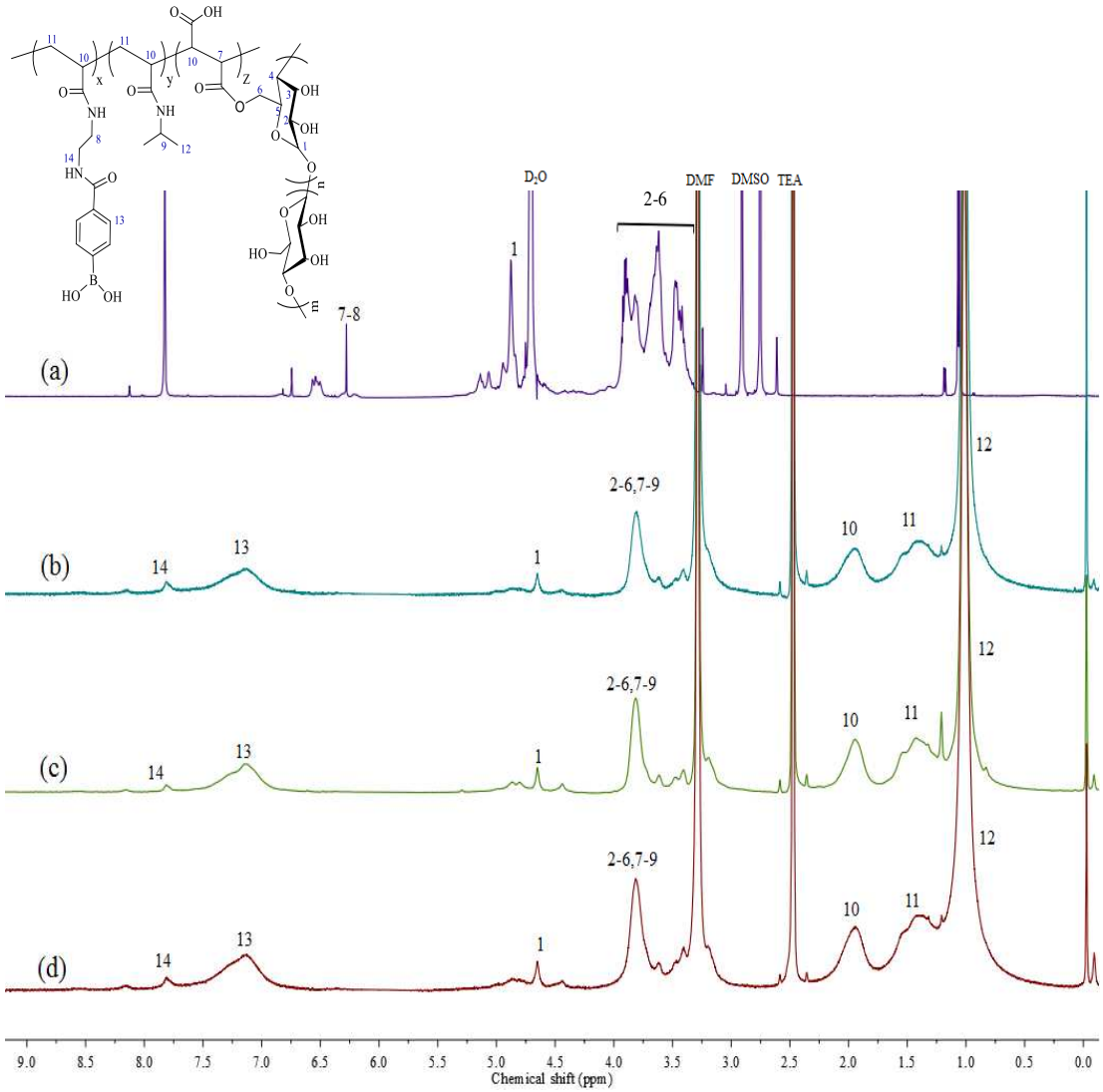

Fig. 4 ^{1}H NMR spectra of (a) Dex-MA, (b) NG1, (c) NG2 and (d) NG3.

283 The X-ray photoelectron spectroscopy (XPS) was used to detect the incorporation of boric acid
284 groups on the nanogel backbone. The spectrum in Fig. S4 shows that the boron atom existed in a
285 few percentages compared to nitrogen, carbon and oxygen atoms. The results are in agreement
286 with that reported by Wu *et al.*, [8] indicating that the DDOPBA was incorporated deeply inside
287 the nanogel particles rather than on their surface [33].
288 The TEM image of the synthesized nanogel (NG2) showed a core-shell structure having an
289 average size of 160 nm (Fig. 5a), and Fig. 5c is the hydrodynamic diameter measured by DLS.
290 It's clearly seen from the insert that the size of NG3 (~ 300 nm) is bigger that the size measured
291 using TEM. However, after the nanogel immersed in glucose and dried in the air, the core-shell
292 structure was fully swollen However, after the nanogel immersed in glucose and dried in the air,
293 the core-shell structure was fully swollen (Fig. 5b).

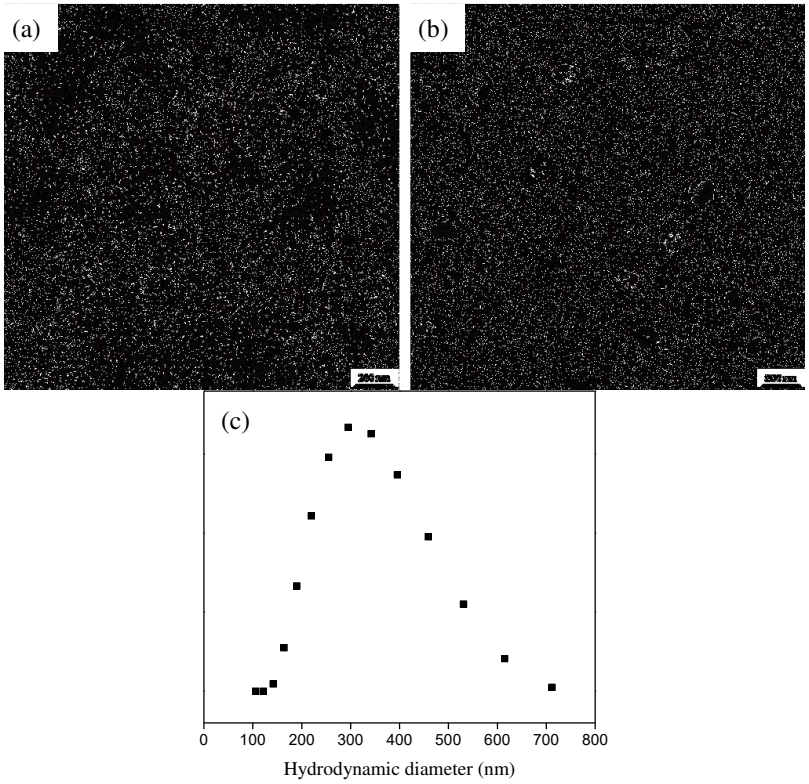

294

295 Fig. 5 (a) TEM image of NG2 (b) TEM image of NG2 after immersion in 5 mg/mL glucose for 6
296 h and (c) the size distribution tested by DLS.

297 TGA has been employed to gain information about the thermal stability of the prepared
298 nanogels. The thermal degradation behaviour was investigated in the range of 100–600 °C under
299 Nitrogen atmosphere. The TGA and DTG overlays of the prepared nanogels are presented in Fig.
300 6. From the TG curves shown in Fig. 6a, it is clear that all nanogels lost weight at a temperature
301 < 130 °C, which was due to the evaporation of water from the nanogel's structure. The addition
302 of Dex-MA as a crosslinker instead of MBA has reduced the thermal stability of the nanogels.
303 The DTG thermograms in Fig. 6b showed two main degradation stages for NG1. The first one in
304 the range of 222-305 °C with a maximum degradation temperature (T_{max}) of 295 °C and the
305 second one in the range of 303-450 °C with a T_{max} of 397 °C. While the DTG of the nanogels
306 prepared using Dex-MA as a crosslinker exhibited three degradation stages in the ranges 174-
307 274 °C, 274-333°C which has been attributed to the degradation of saccharide structure [34]. and
308 333-469 °C which can be assigned to the thermal degradation of the residual polymer backbone
309 [35].

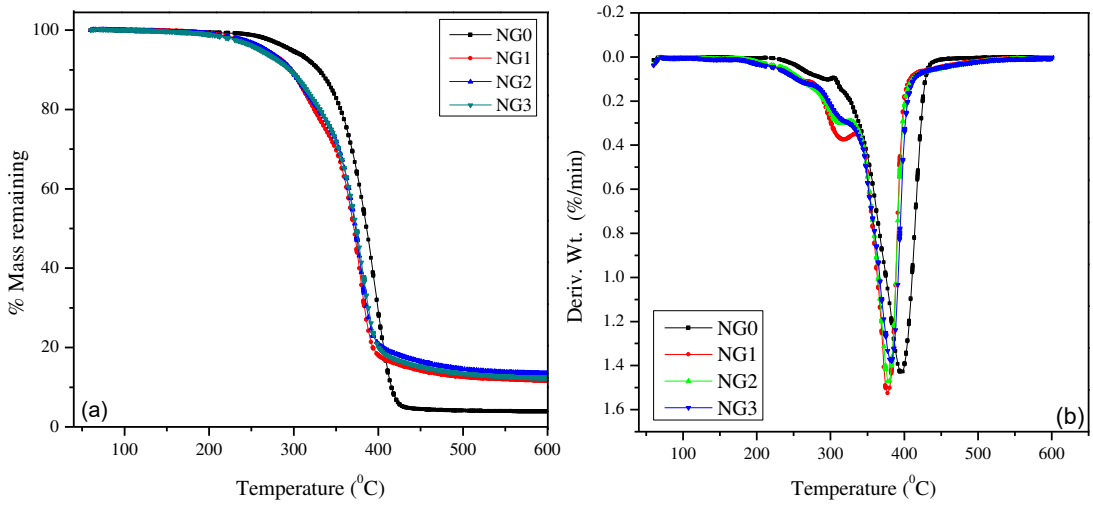

310

311 Fig. 6 (a) TG and (b) DTG curves of the P(NIPAM-*co*-DDOPBA) and P(NIPAM-*co*-Dex-*co*-
312 DDOPBA) nanogels in a nitrogen atmosphere at a heating rate of 10 °C/min.

313 It appears from the curves that the increase in the amount of DDOPBA in the recipe enhanced
314 the thermal stability of the Dex-MA crosslinked nanogels. Also, the interaction between the
315 carboxyl groups with the hydroxyl groups could contribute to the thermal stability of the Dex-
316 MA crosslinked nanogels.

317 **3.4. Glucose-regulated volume phase transition temperature of P(NIPAM-*co*-Dex-*co*-**
318 **DDOPBA) nanogels**

319 It is known that NIPAM at a lower critical solution temperature (LCST) experiences a reversible
320 volume phase transition (VPT) in which the globular form entropically favored water being
321 expelled from the nanogel structure. When the temperature is below 32 °C, the nanogel's
322 hydrophilic/hydrophobic balance shifts to a more hydrophilic nature. As a result, strong
323 hydrogen bonding between the amide groups and the free -COOH groups of maleic acid of the
324 nanogel and water molecule occurs, consequently the nanogel swells. As the temperature
325 increases above the VPTT, the nanogel would become more hydrophobic, and the hydrogen
326 bonding will break, and the nanogel will shrink. Also, the nature of the copolymerised monomers
327 will affect the VPTT of the prepared nanogel [35]. It is expected that the presence of Dex-MA in
328 the nanogel would increase the hydrophilicity due to its hydrophilic nature. Thus, the VPTT of
329 the nanogel would be higher as the hydrogen bonding between the nanogel and water will
330 enhance significantly [18]. For example, the VPTT of NG1 was 30 ºC in PBS, while the VPTT of
331 NG3 was increased to 33 °C, due to the presence of Dex-MA. Fig. 7 illustrates the change in
332 hydrodynamic radius (R_h) of the nanogels as a function of temperature and glucose
333 concentration. It can be observed that the VPTT of the nanogels was shifted right in the presence
334 of glucose. When the nanogel dispersed in 3 mg/mL glucose, the VPTT of NG1 (Fig. 7a) was
335 shifted to 34 °C while that of NG3 was shifted to 37.5 °C. This difference in VPTT is due to the

difference in the levels of hydrophilicity between the nanogels. It can be clearly seen from Fig. 7b that the size of NG2 when it was immersed in PBS shrank to 2.5 folds when the temperature increased from 25 °C to 40 °C due to the internal rearrangement of water and nanogel. For all nanogels, the R_h of the nanogels increased significantly with the increase in glucose concentration. For example, in PBS, NG3 (Fig. 7c) has an average R_h of 692 nm, when immersed in 1, 3, and 5 mg/mL glucose concentration the R_h of NG3 increases by 9%, 29%, and 35%, respectively, which is larger than that reported for AAPBA-based nanogel (6% increase) [23].

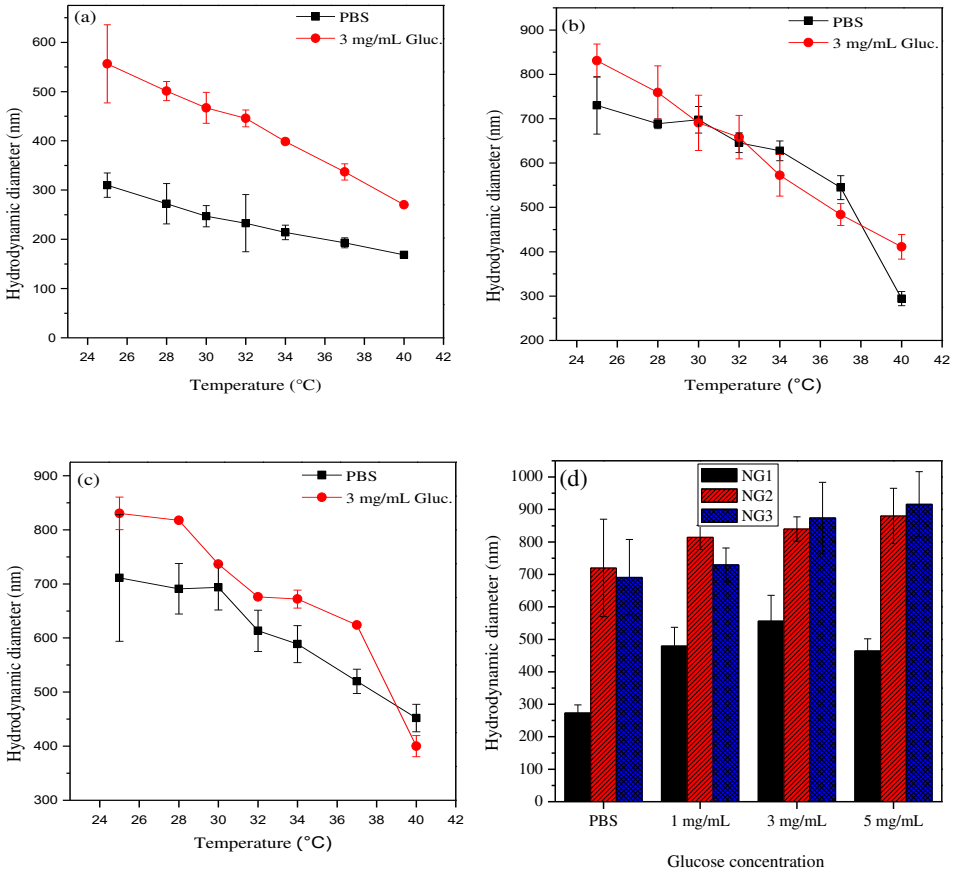

Fig. 7 The variation in R_h of (a) NG1, (b) NG2, and (c) NG3 nanogels as a result of the change in temperature. The nanogel dispersed in 0.1 M PBS pH 7.4, and in 3 mg/mL glucose solution. (**d**) The change in R_h of NG1 and NG3 at different glucose concentrations at 25 ºC.

348 This increment in the nanogel's size can be explained by the enhanced sensitivity of DDOPBA
349 moieties in the nanogel to glucose molecule. Fig. 7d compared the Rh of NG1 and NG3 at
350 different glucose concentration and in both nanogels the Rh was increased with the increase in
351 glucose concentration. It is known that the PBA moieties in an aqueous medium exist in
352 equilibrium between their uncharged form and charged form. When the *p*H of the medium is
353 close to the pKa of PBA, most of the PBA moieties will be changed to the charged form. This
354 form can facilitate the interaction between the PBA moieties and glucose units and form a stable
355 complexation. By increasing the concentration of glucose, more PBA moieties shift to charged
356 form and the hydrophilicity of the polymers will increase. Consequently, the size of the nanogels
357 will increase.

358 **3.5. Insulin release study of P(NIPAM-*co*-Dex-*co*-DDOPBA) nanogels**

359 The permeability and biocompatibility of the nanogel enable it be used for insulin delivery. The
360 thermo-responsive behaviour of the prepared nanogel was used for drug loading and drug release
361 study. Thus, the insulin was encapsulated inside the nanogel at 4°C for 24 h, and the loading
362 capacity (LC) and encapsulation efficacy (EE) for the prepared nanogels were determined using
363 UV-vis spectroscopy. The release study of the loaded insulin was also investigated at 37 °C
364 which was higher than the VPTT of the prepared nanogels. Thus, the nanogel will collapse at this
365 temperature. The EE is increased by increasing the DDOPBA moieties in the nanogel as greater
366 interaction between insulin and DDOPBA moieties will occur. For example, the EE for NG1,
367 NG2 and NG3 were 60 %, 67% and 68 %, while the LC was 14.9 %, 17.7 % and 17.97 %
368 respectively. Fig. 8a depicts the released insulin from the nanogel when incubated with glucose
369 media of different glucose concentrations (0, 1 and 3 mg/mL) at 37 ºC and pH 7.4 for certain
370 time durations. After each time interval, the nanogel was centrifuged, and the adsorption of the

371 release medium was checked, and the medium was changed with a fresh one. The *in vitro* profile
372 of release of insulin from NG3 is shown in Fig. 8. It was observed that the concentration of
373 glucose has a significant effect on the release rate of insulin. The release rate was greater in the
374 presence of glucose solution compared to PBS. The burst release of insulin for NG3 incubated in
375 PBS was only approximately 8 %. This slow release rate of insulin in PBS is mimicking the
376 basal insulin release in the normoglycemic state. In contrast, much faster release of insulin was
377 observed when NG3 was incubated in 1 mg/mL, and 3 mg/mL glucose solutions, where nearly
378 16 % and 28 % of the payload was released in the first hour.

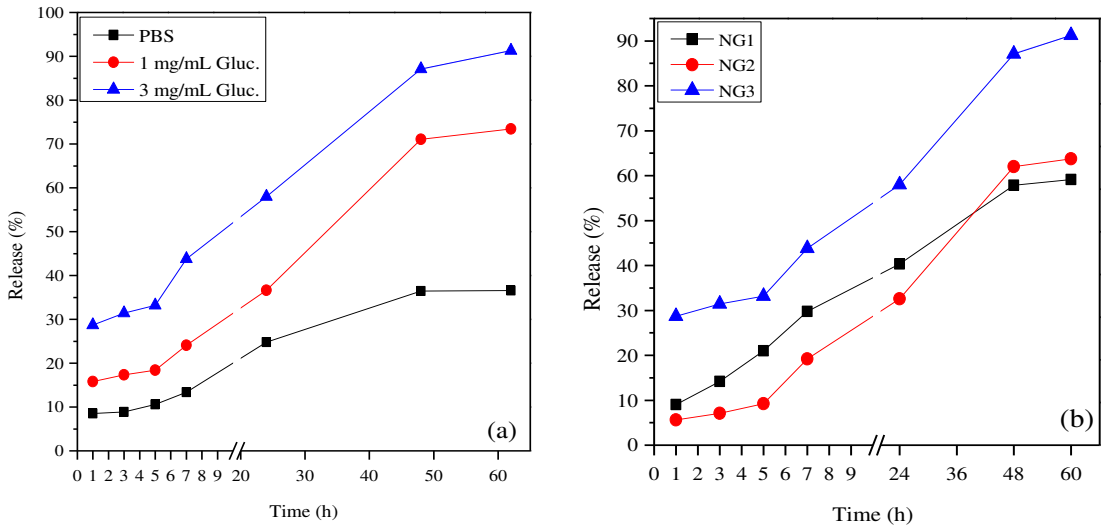

379

380 Fig. 8 *In vitro* release of insulin from (**a**) NG3 at different glucose concentrations (**b**) NG1, NG2
381 and NG3 nanogels in 3 mg/mL glucose dissolved in 0.1 M PBS pH 7.4 at different glucose
382 concentrations.

383 The release of insulin from NG3 was continuously controlled for 48 h, wherein 88 % of
384 insulin was released in 3 mg/mL glucose solution. Fig. 8b compared the release profiles for the
385 prepared nanogels, and it clearly showed that NG3 released more insulin in the first hour than
386 did NG1 and NG2, which was due to the high amount of insulin payload inside NG3 that can
387 generate an impetus diffusion of insulin. Nearly 92 % of the loaded insulin was released from
388 NG3 compared to 64 % for NG1 and 57 % for NG2 when they treated with 3 mg/mL glucose

solution. In this system, DDOPBA enhanced not only on the glucose sensitivity of nanogel, but also sustained the release profile of the encapsulated nanogel. These results suggested that nanogels could be used as injectable insulin-delivery systems due to their small size at physiological conditions and their expected biocompatibility due to the use of Dex-MA as a biodegradable crosslinker [36]. All of these findings indicated that the appropriate monomer in a rational design could provide a sustained release of the drug under physiological conditions. Scheme 3 demonstrated the procedure of insulin loading and insulin release from the nanogel. The nanogel forms a core-shell structure at temperature ≤ VPTT and pH ≤ pKa of PBA moiety. Under these conditions, a PBA moiety forms the core due to its hydrophobic nature, while NIPAM and dextran form the hydrated shell. When the insulin-loaded nanogels were immersed in the release medium containing glucose at pH 7.4 and temperature 37 ºC, the PBA get protonated and bind to glucose increasing the charge density and the hydrophilicity of the nanogel, as a consequence, the nanogel swells and also VPTT shifts near 37 ºC. This glucose induced size change will enhance the release of insulin from the nanogel.

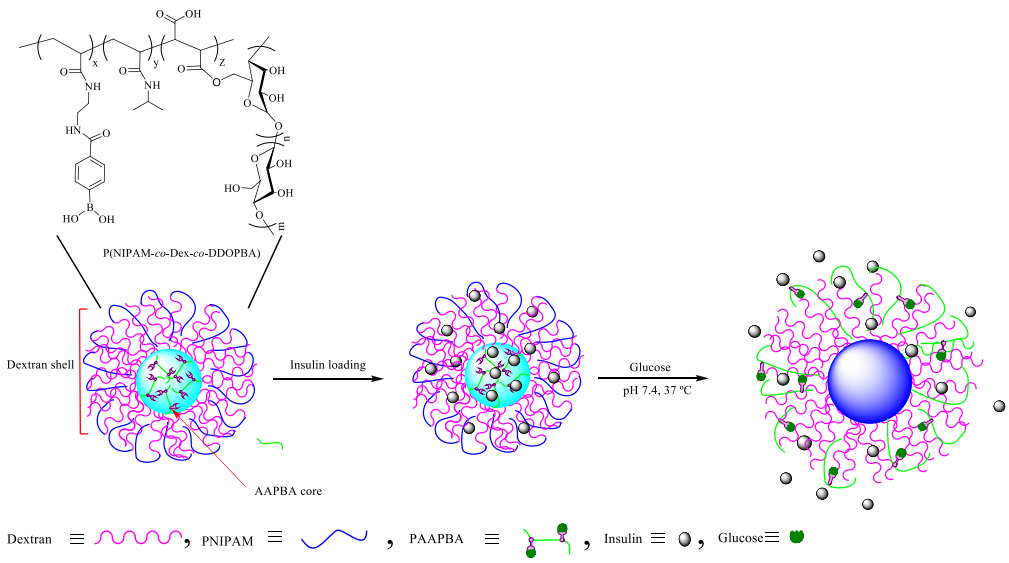

Scheme 3 Schematic model of the glucose-induced insulin delivery of the nanogel.

4. Conclusion

Three glucose-responsive nanogels of poly(N-isopropylacrylamide-co-dextran-grafted maleic acid-co-4-(1,6-dioxo-2,5-diaza-7-oxamyl) phenylboronic acid) nanogels, named as NG1, NG2 and NG3 were prepared using free radical polymerization. The structures of these nanogels were characterized by 1H NMR. The shape and size of the nanogels were characterized using TEM and DLS. The thermal stability of the prepared NGs was investigated using TG and DTG techniques. The VPTT was located by measuring the change in the nanogel's size via DLS. The glucose-induced insulin delivery from the nanogels was studied by UV-vis spectrometer The nanogel's swelling was significant when immersed in glucose solutions at physiological temperature, and the insulin-loaded NGs showed high dependence on glucose concentration at physiological pH and temperature. These NGs can be suitable for insulin delivery systems as the response to glucose alterations occurs under physiological pH and temperature.

Acknowledgement

Financial support from the Science and Technology program of Zhejiang Province (2019C030637) and the Fundamental Research Funds for the Central Universities (2019FZA4022) are gratefully acknowledged.

Reference

[1] J. Xie, A. Li, J. Li, Advances in pH-sensitive polymers for smart insulin delivery, Macromol. Rapid. Commun. 38 (2017) 1700413, 1-14.

[2] X. Xu, H. Shang, T. Zhang, P. Shu, Y. Liu, J. Xie, D. Zhang, H. Tan, J. Li, A stimuli-responsive insulin delivery system based on reversible phenylboronate modified cyclodextrin with glucose triggered host-guest interaction, Int. J. Pharm. 548 (2018) 649-658.

[3] Q. Huang, L. Wang, H. Yu, K. Ur-Rahman, Advances in phenylboronic acid-based closed-loop smart drug delivery system for diabetic therapy, J. Control. Release 305 (2019) 50-64.

429 [4] S. Nayak, H. Lee, J. Chmielewski, L.A. Lyon, Folate-mediated cell targeting and cytotoxicity
430 using thermoresponsive microgels, J. Am. Chem. Soc.126 (2004) 10258-10259.

431 [5] W.L.A. Brooks, C.C. Deng, B.S. Sumerlin, Structure–Reactivity Relationships in Boronic
432 Acid–Diol Complexation, ACS Omega 3(12) (2018) 17863-17870.

433 [6] D. Roy, J.N. Cambre, B.S. Sumerlin, Sugar-responsive block copolymers by direct RAFT
434 polymerization of unprotected boronic acid monomers, Chem.Commun. (Cambridge, United
435 Kingdom) (2008) 2477-2479.

436 [7] D. Roy, B.S. Sumerlin, Glucose-sensitivity of boronic acid block copolymers at physiological
437 pH, ACS Macro Lett. 1 (2012) 529-532.

438 [8] Z. Wu, X. Zhang, H. Guo, C. Li, D. Yu, An injectable and glucose-sensitive nanogel for
439 controlled insulin release, J. Mater. Chem. 22 (2012) 22788-22796.

440 [9] A. Matsumoto, S. Ikeda, A. Harada, K. Kataoka, Glucose-responsive polymer bearing a
441 novel phenylborate derivative as a glucose-sensing moiety operating at physiological pH
442 conditions, Biomacromolecules 4 (2003) 1410-1416.

443 [10] W. Wu, N. Mitra, E.C.Y. Yan, S. Zhou, Multifunctional hybrid nanogel for integration of
444 optical glucose sensing and self-regulated insulin release at physiological pH, ACS Nano 4
445 (2010) 4831-4839.

446 [11] D. Shiino, Y. Murata, A. Kubo, Y.J. Kim, K. Kataoka, Y. Koyama, A. Kikuchi, M.
447 Yokoyama, Y. Sakurai, T. Okano, Amine containing phenylboronic acid gel for glucose-
448 responsive insulin release under physiological pH, J. Control .Release 37 (1995) 269-276.

449 [12] M. Dowlut, D.G. Hall, An improved class of sugar-binding boronic acids, soluble and
450 capable of complexing glycosides in neutral water, J. Am. Chem. Soc. 128 (2006) 4226-4227.

451 [13] A. Matsumoto, M. Tanaka, H. Matsumoto, K. Ochi, Y. Moro-oka, H. Kuwata, H. Yamada,
452 I. Shirakawa, T. Miyazawa, H. Ishii, K. Kataoka, Y. Ogawa, Y. Miyahara, T. Suganami,
453 Synthetic “smart gel” provides glucose-responsive insulin delivery in diabetic mice, Sci. Adv. 3
454 (2017) 1-13.

455 [14] C. Zhang, M.D. Losego, P.V. Braun, Hydrogel-based glucose sensors: effects of
456 phenylboronic acid chemical structure on response, Chem. Mater. 25 (2013) 3239-3250.

457 [15] A. Matsumoto, T. Ishii, J. Nishida, H. Matsumoto, K. Kataoka, Y. Miyahara, A synthetic
458 approach toward a self-regulated insulin delivery system, Ang. Chem. Int. Ed. 51 (2012) 2124-
459 2128.

460 [16] A. Matsumoto, R. Yoshida, K. Kataoka, Glucose-responsive polymer gel bearing
461 phenylborate derivative as a glucose-sensing moiety operating at the physiological pH,
462 Biomacromolecules 5 (2004) 1038-1045.

463 [17] K. Nagahama, Y. Mori, Y. Ohya, T. Ouchi, Biodegradable nanogel formation of
464 polylactide-grafted dextran copolymer in dilute aqueous solution and enhancement of its stability
465 by stereocomplexation, Biomacromolecules 8 (2007) 2135-2141.

466 [18] J. A. Cade, M. J. A. van Luyn, L. A. Brouwer, J. A. Plantinga, P. B.van Wachem, C. J.
467 Groot, W. Otter, W. E. Hennink., In vivo biocompatibility of dextran-based hydrogels, J.
468 Biomed. Mater. Res. 50 (2000) 397-404.

469 [19] L. Li, Z. Bai, P.A. Levkin, Boronate-dextran: An acid-responsive biodegradable polymer for
470 drug delivery, Biomaterials 34 (2013) 8504-8510.

471 [20] X. Zhang, D. Wu, C.C. Chu, Synthesis and characterization of partially biodegradable,
472 temperature and pH sensitive Dex-MA/PNIPAAm hydrogels, Biomaterials 25 (2004) 4719-
473 4730.

474 [21] K.S. Hee, W.C.Youb, C.C.Chang, Synthesis and characterization of dextran-maleic acid
475 based hydrogel, J. Biomed. Mater. Res. 46 (1999) 160-170.

476 [22] A. Sinha, A. Chakraborty, N.R. Jana, Dextran-gated, multifunctional mesoporous
477 nanoparticle for glucose-responsive and targeted drug delivery, ACS Appl. Mater. Interfaces 6
478 (2014) 22183-22191.

479 [23] J.L. Ifkovits, J.A. Burdick, Review: photopolymerizable and degradable biomaterials for
480 tissue engineering applications, Tissue Eng. 13 (2007) 2369-2385.

481 [24] M.P. Stephen., S. John, Immobilized RGD peptides on surface-grafted dextran promote
482 biospecific cell attachment, J. Biomed. Mater.Res. 56 (2001) 390-399.

483 [25] Y. Zhang, Y. Guan, S. Zhou, Synthesis and volume phase transitions of glucose-sensitive
484 microgels, Biomacromolecules 7 (2006) 3196-3201.

485 [26] N. Inomoto, N. Osaka, T. Suzuki, U. Hasegawa, Y. Ozawa, H. Endo, K. Akiyoshi, M.
486 Shibayama, Interaction of nanogel with cyclodextrin or protein: Study by dynamic light
487 scattering and small-angle neutron scattering, Polymer 50 (2009) 541-546.

488 [27] M.M. Bradford, A rapid and sensitive method for the quantitation of microgram quantities
489 of protein utilizing the principle of protein-dye binding, Anal. Biochem. 72 (1976) 248-254.

490 [28] J. Cao, S. Liu, Y. Chen, L Shi, Z. Zhang, Synthesis of end-functionalized boronic acid
491 containing (*co*) polymers and their bioconjugates with rodlike viruses for multiple responsive
492 hydrogels, Polym. Chem. 5 (2014) 5029-5036.

[29] J.A. Faniran, H.F. Shurvell, Infrared spectra of phenylboronic acid (normal and deuterated) and diphenyl phenylboronate, Can. J. Chem. 46 (1968) 2089-2095.

[30] M.S. S. Manja Kurecic, Karin Stana-Kleinschek, UV polymerization of poly (*N*-isopropylacrylamide) hydrogel, Mater. Technol. 46 (2012) 87-91.

[31] W. Hyk, M. Ciszkowska, Preparation and electrochemical characterization of poly(*N*-isopropylacrylamide-*co*-acrylic acid) gels swollen by nonaqueous solvents: Alcohols, J. Phy. Chem. B 106 (2002) 11469-11473.

[32] H. Peng, X. Ning, G. Wei, S. Wang, G. Dai, A. Ju, The preparations of novel cellulose/phenylboronic acid composite intelligent bio-hydrogel and its glucose, pH-responsive behaviors, Carbohydr. Polym.195 (2018) 349-355.

[33] P. Hazot, T. Delair, A. Elaïssari, J.P. Chapel, C. Pichot, Functionalization of poly(*N*-ethylmethacrylamide) thermosensitive particles by phenylboronic acid, Colloid Polym. Sci. 280 (2002) 637-646.

[34] H.F. Zhang, H. Zhong, L.l. Zhang, S.b. Chen, Y.J. Zhao, Y.l. Zhu, Synthesis and characterization of thermosensitive graft copolymer of *N*-isopropylacrylamide with biodegradable carboxymethylchitosan, Carbohydr. Polym. 77 (2009) 785-790.

[35] L. Sun, X. Zhang, C. Zheng, Z. Wu, X. Xia, C. Li, Glucose- and temperature-responsive core-shell microgels for controlled insulin release, RSC Advances 2 (2012) 9904-9913.

[36] Z. Gu, A.A. Aimetti, Q. Wang, T.T. Dang, Y. Zhang, O. Veiseh, H. Cheng, R.S. Langer, D.G. Anderson, Injectable Nano-Network for Glucose-Mediated Insulin Delivery, ACS Nano 7 (2013) 4194-4201.